Individual tree detection and crown segmentation based on metabolic theory from airborne laser scanning data

Honglu Xin,[a,b] Yadvinder Malhi,[b] David A. Coomes,[c] Yi Lin,[a] Baoli Liu,[b] Qiuli Yang,[d] and Alexander Shenkin[b,*]

[a]Peking University, Institute of Remote Sensing and Geographic Information Systems, School of Earth and Space Science, Beijing, China

[b]University of Oxford, Environmental Change Institute, School of Geography and the Environment, Oxford, United Kingdom

[c]University of Cambridge, Department of Plant Sciences, Forest Ecology and Conservation Group, Cambridge, United Kingdom

[d]Chinese Academy of Sciences, Institute of Botany, State Key Laboratory of Vegetation and Environmental Change, Beijing, China

Abstract. Laser scanning technology has enabled to study three-dimensional (3D) structures in forests. For example, airborne laser scanning (ALS) point cloud has been applied to detect individual trees and segment tree crowns. However, the accuracy of such approach remains a challenge because of the intersected crowns and complicated understories. We developed a metabolic theory-based algorithm for individual tree detection and crown segmentation from ALS data. The algorithm is composed of two parts, of which one is an unscaled transporting distance-based top-to-bottom detection approach, and the other is a scaled transporting distance-based segmentation approach. The unscaled transporting distance for detection is the absolute distance from tree root to crown and then to ALS point based on the tree structure models, whereas the scaled transporting distance for segmentation is the unscaled distance that is scaled by an initial tree height obtained during detection. This is based on a basic metabolic theory that vascular plants tend to minimize the material transporting distance from root to leaves. Hence, seven types of materials transporting distance models were built based on monopodial branching structure or crown-centered structure. The performance of the proposed approach was then further examined and compared with two typical canopy height model-based approaches and one typical point cloud-based approach, taking forest in Oxfordshire, UK, as a case study. The results showed that our approach can reach a recall of 1.00, a precision of 0.96, and an F-score of 0.98 and can reach to much higher accuracy for tree height ($R^2 = 0.8045$) than the comparison approaches ($R^2 < 0.2$) in the study plot. One of the main reasons that led to such low accuracy of comparison approaches is much overestimation of understory height with a mean error that is 2.9 times higher than that of our approach on average. Furthermore, ALS point-to-point level accuracy assessment shows 9.7% more ALS points were truly assigned in our approach than that of comparison approaches. It is noticed that the algorithm presented is not sensitive to the two key parameters: p (a percentage determining the threshold of unscaled transporting distances) ranging from 32.0% to 34.0% and λ (the proportion between the assumed crown center height and tree height) ranging from 0.70 to 0.90 based on our data set. Such high accuracy of our approach can greatly improve detections of individual tree and crown segmentation, especially in delineating understories in complex-structured forest. [DOI: 10.1117/1.JRS.15.034504]

Keywords: airborne laser scanning; individual tree detection; crown segmentation; metabolic theory; understory.

Paper 210207 received Apr. 3, 2021; accepted for publication Jun. 24, 2021; published online Jul. 9, 2021.

*Address all correspondence to Alexander Shenkin, alexander.shenkin@ouce.ox.ac.uk

1931-3195/2021/$28.00

1 Introduction

In the last decade, airborne laser scanning (ALS), a state-of-the-art technology for remote sensing, has rapidly become an effective tool for forest survey due to its higher performance in obtaining three-dimensional (3D) structure parameters of trees in large areas.[1,2] Mapping terrain and trees using ALS data produces information such as estimation of tree size, leaf area index, and biomass. This is especially useful in a survey of complex forest, where field inventory could be time-consuming and with limited information.[3,4]

Tree stem position, height, and crown size can be derived once individual tree crowns (ITCs) are segmented from ALS point cloud.[5–8] Tree detection and segmentation algorithms are based on either the two-dimensional (2D) canopy height model (CHM) or raw 3D ALS points.[9,10] CHM can be used for delineating tree crowns by finding local maxima within a fixed or variable window, but it loses part of understory information when converting from 3D points to a 2D raster image.[11–14] Approaches delineating ITCs directly from ALS point cloud, e.g., *k*-means cluster approach,[15] adaptive clustering approach,[16] and regional growing approach,[17,18] showed great potential in delineating trees, but there is also obvious undersegmentation of understory because ALS points from lower canopies may be incorrectly assigned to midstory or overstory. Meanwhile, methods combining both laser scanning data and other remote sensing data for delineating ITCs, e.g., multispectral[19,20] and hyperspectral data,[18,21,22] also greatly succeeded in segmentation, but they need more kinds of source data.

ITCs segmentation approach inspired by ecological theories has been proposed in recent years and is proved to be a practical way for delineating ITCs from laser scanning data.[23–25] In essence, assigning a laser scanning point to a tree is similar to assigning a piece of leaf to a tree. The assignment could be made by a universal rule of a metabolic transporting theory that vessel architecture plants tend to maximize the efficiency of transporting nutrition from root to leaves, and one way to implement is to minimize the path distance, which is called transporting distance.[26–28] This type of assignment could greatly remove the potential influence by overstories during the delineation of understories, as overstories have the relative longer transporting distances. Moreover, there is a universal law that nutrition transporting efficiency is directly proportional to the radius of stems or branches, thus, the relative transporting distance is inversely proportional to the radius of stems or branches, more broadly, to the size of tree. The transporting distances could be scaled by the size of tree, and the scaling factor was proved to be close to two-third power of tree size (e.g., tree height).[29–31] For segmenting individual trees from terrestrial and mobile laser scanning data, Tao et al.[25] developed a metabolic transporting distance (MTD)-based shortest path algorithm. Metabolic scaling theory was also applied to reduce the frequency of commission error in variable regional local maxima algorithm segmenting trees from ALS point cloud,[23] but it was based on CHM and had the potential of missing understory.[24,32] Therefore, the metabolic transporting theory shows huge potential in directly delineating understories from point cloud, which is covered by overstories. However, research in applying MTD to individual tree segmentation using ALS data is still rare, which is due to the challenge of tracking nutrition transporting path from the relative sparse ALS point cloud.

To fill this technical gap, we developed a new algorithm using MTD theory for individual tree detection and crown segmentation based on ALS point cloud. To trace material transporting path, we employed seven types of monopodial structure- and crown center-based models to calculate transporting distance from root to points and took factors related to initial tree height or presumed crown center height as the scaling factor to scale the distance. To reduce common overestimation of understory size (see Secs. 3.3 and 4), we used the scaled distance to allocate ALS points. The specific objectives are (1) to develop an unscaled transporting distance-based top-to-bottom approach for detecting individual trees and (2) to develop a scaled transporting distance-based approach for segmenting crowns. The unscaled distance was tracked based on the tree structure models during detection due to the absence of tree height information, and scaled distance was tracked during segmentation as the initial tree height was already obtained in detection. Moreover, three common-used typical CHM- and raw point cloud-based ITCs segmentation approaches were also implemented in parallel for comparison in the plot, and we evaluated the results at both tree level and ALS point-to-point level. Results of three canopy layers show

that, compared with comparison approaches, our approach is better in delineating tree, especially for understories that are difficult to segment.

2 Materials and Methods

2.1 *Study Area and Data Collection*

The study area is a 1-ha plot in a deciduous forest located in Wytham Woods (1°20′W, 51°47′N), Oxfordshire, UK. The plot is dominated by *Acer pseudoplatanus* (Sycamore, 364 individuals, 69.6%), *Fraxinus excelsior* (Ash, 53 individuals, 10.1%), *Corylus avellana* (Hazel, 33 individuals, 6.3%), *Quercus robur* (Oak, 23 individuals, 4.4%), *Crataegus monogyna* (Hawthorn, 17 individuals, 3.3%), and other species (33 individuals, 6.3%). The forest is part of the ForestGEO global network forest inventory plots and is managed by the University of Oxford.[33,34] In this area, the mean annual temperature is 10°C with a mean annual rainfall of 726 mm.

Terrestrial laser scanning (TLS) data were collected with a RIEGL VZ-400 terrestrial laser scanner at multiple scanning locations in leaf-off (December 2015 and January 2016) condition.[35] Reflective targets were placed during the scan to conjunct all investigated locations. According to the manual segmentation for TLS, the tree point density was about 11,000 pts/m^2. ALS data with a density of 6.0 pts/m^2 were collected with a Leica ALS-50 II scanner in leaf-on (June 2014) condition in an 18-ha area containing the 1-ha plot.[33,34] The filtering results suggested that the tree point density was 5.4 pts/m^2.

The TLS detected 523 individual trees in the 1-ha plot, of which the average tree height is 15.42 m, the average crown width is 6.18 m. To assess the accuracy of detecting and segmenting understories of our approach, we further subdivided the trees based on tree height into three layers, which are understory (tree height under 10 m), midstory (between 10 and 20 m), and overstory (above 20 m), as shown in Table 1. Performance assessment of the three layer's detection and segmentation was carried out separately.

2.2 *Data Preprocessing and Point Cloud Matching*

523 individual trees and corresponding TLS points were manually extracted from the 1-ha TLS data under careful visual inspection. The maximum TLS point number of individual tree was 5,780,668, the minimum was 2224, with an average value of 213,986. Note that the point number differences of individual trees were caused by the differences of tree size. For each individual tree, we took the lowest TLS point as the tree root location, the highest TLS point as the treetop, and the z-coordinate difference of top and bottom points as tree height [Fig. 1(a)]. Similarly, we took east–west distance of the easternmost and westernmost points of an individual tree as the east–west direction crown width and the north–south distance of the northernmost and southernmost points as the north–south direction crown width [Fig. 1(b)]. The crown width of a tree is the average of east–west and north–south direction crown widths.

We processed ALS point cloud as following. After we detected and removed the spurious points, we classified all the points as ground points and tree points using an improved

Table 1 Information of three canopy layers of trees in the 1-ha plot. The statistics were based on manually segmented TLS data, and the TLS data were used for validation of the algorithm. Note that the trees with height shorter than 2.0 m were not counted.

Layer	Tree height (m)	Tree number	Mean height (m)	Mean crown width (m)
Overstory	≥20	178	22.66	8.70
Midstory	10 to 20	198	15.21	5.75
Understory	≤10	147	6.92	3.73
All trees	2.23 to 30.19	523	15.42	6.18

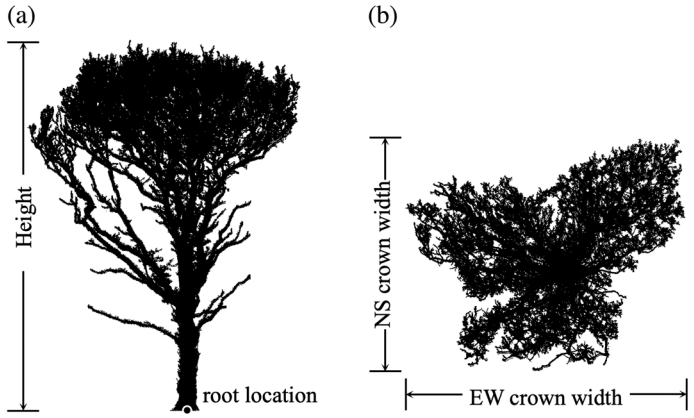

Fig. 1 Schematic diagram of extracting (a) root location, and height and (b) crown width from TLS point cloud after manual visual inspection.

progressive triangulated irregular network densification filtering algorithm[36] in the LiDAR360 software.[37] The parameters of the algorithm, iterative angle and iterative distance, were set as the common value of 30 deg and 1.6 m, respectively. The maximum slope was set as 36 deg according to the census data. Then, we extracted digital surface model (DSM) from tree points and digital elevation model (DEM) from ground points.[38,39] Then, CHM, which was used for comparison approaches, was produced by subtracting DEM from DSM.[40–42] Next, the tree points were normalized by subtracting the elevation value of corresponding DEM pixel from the z-coordinate of point. Note that we implemented detection and segmentation algorithms on normalized tree points. The above processes and implementation of the three comparison approaches were processed in the LAStools[43] and LiDAR360 software,[37] and all the following processes were analyzed using Python language.[44]

The 1-ha TLS and corresponding ALS data were accurately reprojected to the same projection coordinate system. It is commonly recognized that an ALS point and its spatial nearest TLS point are most likely from the same individual tree, and we assigned each ALS point to the tree with the spatial nearest TLS point. The truly assigned ALS point cloud was then obtained, which is called true ALS, and it is used for point-to-point level assessment. Similar to TLS (Fig. 1), we extracted height and crown width of 523 individual trees based on ALS point cloud (Fig. 2).

Trees that fell below the 1:1 line in Figs. 2(a) and 2(b) indicated the lack of understory ALS points.[45,46] 58 trees were not assigned with any ALS point due to the relative sparse point density [Fig. 2(c)] and fell at the bottom of the scatter diagrams in Figs. 2(a) and 2(b). The average height and crown width of these trees from TLS data were 7.13 and 2.88 m, respectively, which

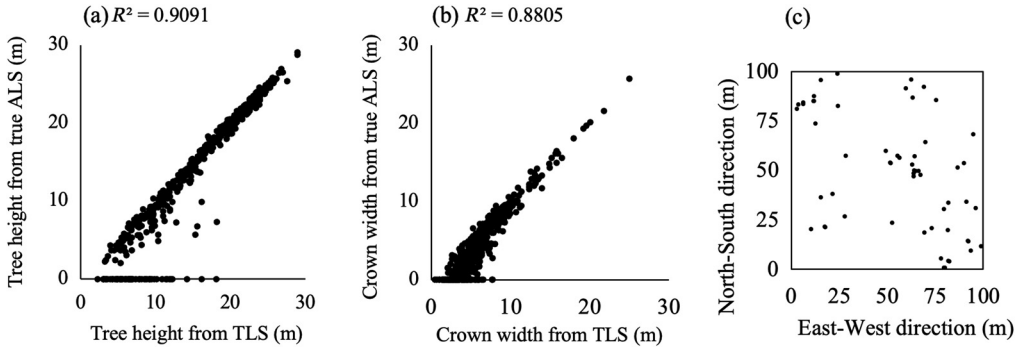

Fig. 2 Relationship between TLS- and true ALS-derived (a) tree height and (b) crown width. Coefficients of determination (R^2) are provided. The 58 dots that fell on the x-axis are the understories, which were not assigned with any ALS point and were marked the height as 0 m, the crown width as 0 m. (c) Spatial distribution of 58 understory trees that were not assigned with any ALS point. Note that the true ALS is the truly assigned data.

indicated they were understories, whereas the average values of all the 523 trees were 15.42 and 6.18 m, respectively.

Values of ALS-based tree height and crown width were expectedly underestimated compared with TLS (Fig. 2), and this indicated that there is always underestimation no matter how well the detection and segmentation approaches are. Therefore, we used tree height and crown width derived from true ALS as the true values for a more accurate accuracy assessment, instead of those from TLS.

2.3 *Detection Approach*

The proposed algorithm contains two main steps: first detecting individual trees and second segmenting tree crowns. As tree heights were unknown during detection, we employed unscaled transporting distance for tree detection; conversely, tree heights were known during segmentation, so we employed scaled transporting distance for crown segmentation. As shown in Fig. 3, ALS point P_1 was truly assigned to tree 2, according as the unscaled transporting distance of P_1 along stem and branch for tree 1, $a_1 + c_1$, is longer than that for tree 2, $a_2 + c_2$. This allowed the ALS points with relative low height would be much less likely to be falsely assigned to overstories, especially for the points belonging to understories. Also, this avoiding further overestimation of understories tree height and overestimation of overstories crown width. This the reason why the transporting distance-based algorithm performs well in detecting understories, and the statistical analysis of understories is given in Sec. 3.3.

The unscaled transporting distance-based detection approach is based on the top-to-bottom technique. Let U_i denote the set of current points to be assigned and i denote the number of detected trees. The pseudocode of detection approach is as following (Algorithm 1).

The key point of the detection approach based on crown center-structured unscaled transporting distance is to trace unscaled distance D_{unscaled} and unscaled distance threshold $D_{\text{unscaled}}(z, p)$.

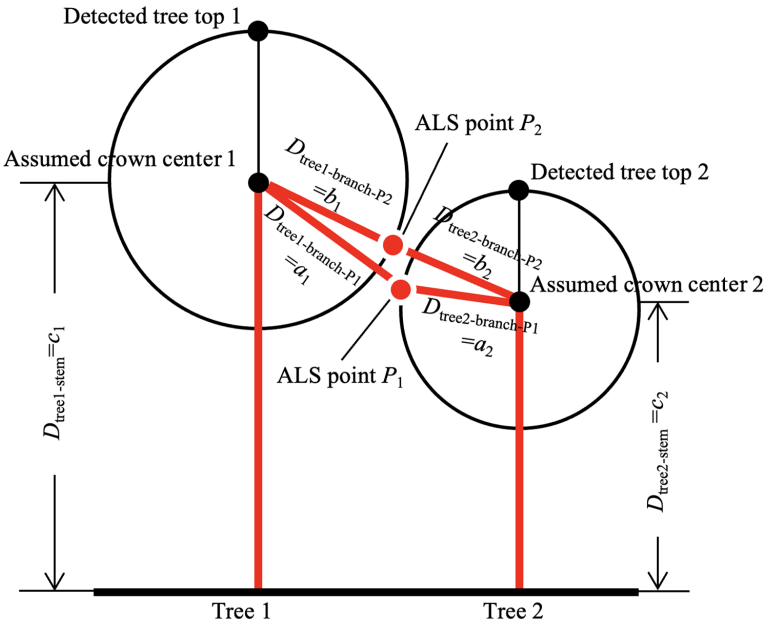

Fig. 3 Schematic diagram of MTD based on crown center structure. a_1 and a_2 are the distances from ALS point P_1 to crown center of trees 1 and 2, respectively. b_1 and b_2 are the distances from ALS point P_2 to crown center of trees 1 and 2, respectively. c_1 and c_2 are the distances along stems. The ALS point is assigned to the tree with shortest transporting distance. Note that we used a parameter λ, where λ = tree center height/tree height, to determine the crown center, and a pilot test of a series of values of λ was conducted.

Algorithm 1 The pseudocode of detection approach.

```
INITIALIZE total tree number i to 0
WHILE U_i is not empty
  FOR each ALS point in U_i
    IF the ALS point is the highest point in U_i
      i = i + 1
      SET the ALS point as the treetop of tree i   # When the point's xy-coordinates are the location of tree i, z-coordinate is the height of tree i.
        FOR each ALS point in U_i
          IF D_unscaled is smaller than D_unscaled(z, p)   # D_unscaled is the unscaled transporting distance of the point regarding to tree i, and D_unscaled(z, p) is an essential threshold varying according to the parameter p and the z-coordinate of the point.
            This point is assigned to tree i
            This point is removed from U_i
          ENDIF
    ENDIF
ENDWHILE
```

D_{unscaled} was set as the distance from ALS point to crown center, and the crown center height was set as λ times of tree height, where parameter λ was the proportion between the crown center height and tree height.

According to the pseudocode of detection approach, there will be much fewer detected individual trees, because the upper boundary will accommodate points that do not belong to the tree. Therefore, we came up with the percentage line with a parameter p, a threshold line between the lower and upper boundaries. This is to proportionally move the upper boundary to left. When the proportion is p, the area between lower and upper boundaries was narrowed, thus "restricts" the number of ALS points assigned to trees, and results in detections of more trees. Results in Table 3 showed that only 63 trees were detected without the restriction of parameter p (i.e., $p = 100.0\%$), whereas 529 trees were detected with parameter $p = 34.0\%$; however, the real tree number in the plot is 523.

$D_{\text{unscaled}}(z, p)$ is a distance threshold function, in which value at the height of z is the value of the percentage line at that height, providing a reference for judgment whether an ALS point belongs to an individual tree. More trees will be detected if the value of p is smaller; less trees will be detected if the value of p is higher.

$D_{\text{unscaled}}(z, p)$ is determined by training data that were explored in Fig. 4, in which the scatter diagram of unscaled transporting distance and z-coordinate of true ALS points showed clear boundaries (red dashed lines). Unscaled transporting distance is the distance between ALS point and the tree crown center, and the crown center was determined by parameter λ, where λ = tree center height/tree height. λ was tested with value from 0.1 to 0.9, and 0.8 was proved to be the optimal value according to tree level assessment with recall, precision, and F-score. $b_{\text{lower}}(z)$ and $b_{\text{upper}}(z)$ are the lower and upper boundary functions that outline the clear lower [left dashed line in Fig. 4(b)] and upper boundaries (right dashed line) of all the points. The lower boundary can be simplified as a piecewise function, fixed by points (0.9, 0.0), (0.7, 11.6), (0.8, 16.2), (2.8, 26.0), and (5.4, 30.0), and the upper boundary can be also simplified as a piecewise function, fixed by points (17.6, 0.0), (12.8, 11.6), (17.6, 16.2), (12.6, 26.0), and (8.5, 30.0). We set that $D_{\text{unscaled}}(z, p) = p \times [b_{\text{upper}}(z) - b_{\text{lower}}(z)] + b_{\text{lower}}(z)$, where $D_{\text{unscaled}}(z, p)$ (solid red line) is

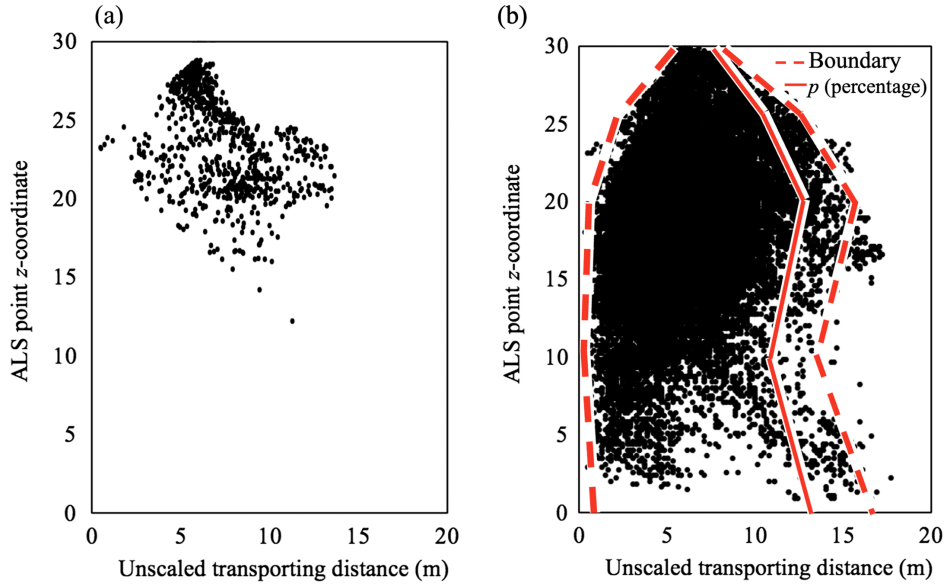

Fig. 4 Scatter diagrams of unscaled transporting distance and *z*-coordinate of points based on true ALS. (a) An example tree with 846 ALS points, tree height is 28.76 m. (b) The overlay of ALS points of all 523 trees shows clear boundaries (red dashed lines), the red solid line is a percentage line determined by parameter *p*.

a threshold function setting to judge whether an ALS point belongs to an individual tree. p, ranging from 0% to 100%, is a percentage threshold determining $D_{\text{unscaled}}(z, p)$.

For example, if p was set as 80.0%, then the threshold function $D_{\text{unscaled}}(z, p)$ can be a piecewise function fixed by points (14.3, 0.0), (10.4, 11.6), (14.2, 16.2), (10.6, 26.0), and (7.9, 30.0). p is a crucial parameter determining the number of detected trees, for example, detection approach when percentage line parameter $p = 80.0\%$ detected fewer individual trees than that when $p = 50.0\%$.

By applying the unscaled transporting distance-based top-to-bottom approach, data were obtained including the detected i trees, their heights, locations, and detection-based assigned ALS points. To segment tree crowns, an initial assignment could be done during detection. However, the assignment accuracy needs to be further improved and was done by applying the approach below.

2.4 *Segmentation Approach*

The unscaled transporting distance-based algorithm has the potential of false assignment. As shown in Fig. 3, ALS point P_2 belonging to tree 1 would be falsely assigned to tree 2, according as the unscaled transporting distance of P_2 along stem and branch for tree 1, $b_1 + c_1$, is longer than that for tree 2, $b_2 + c_2$. Thus, aiming at improving assignment accuracy, a scaled transporting distance-based crown segmentation approach was developed to reassign ALS points. This approach was designed according to an ecological theory that taller trees always have thicker stems and branches, which greatly increase transporting efficiency.[31,47] Note that the segmentation approach has no ability to detect tree stems, so individual tree detection has to be done before crown segmentation, which was processed based on tree locations and heights extracted from detection, and the steps are below:

1. For an ALS point, calculate the scaled transporting distance from the ALS point to all trees.
2. Reassign the point to the tree with the shortest scaled transporting distance.
3. Iterate through all ALS points as steps 1 and 2.

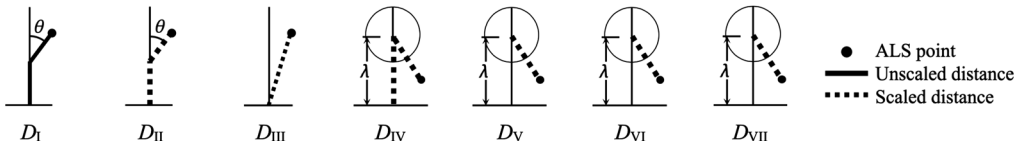

Fig. 5 Schematic diagrams of seven transporting distances calculation methods. θ was the intersection angle between branch and stem, ranging from 0 deg to 90 deg.[48,49] D_{I} and D_{II} are based on monopodial structure, whereas D_{IV}, D_{V}, D_{VI}, and D_{VII} are based on crown center structure.

"Reassigning" in segmentation is distinct from "assigning" in detection approach. Seven transporting distance calculating methods were developed, namely D_{I}, D_{II}, D_{III}, D_{IV}, D_{V}, D_{VI}, and D_{VII} (Fig. 5). The schematic diagrams of the seven methods are shown in Fig. 5.

D_{I} is the unscaled distance along stem and branch based on monopodial structure.

D_{II} is the scaled distance along branch based on monopodial structure, scaled by tree height.

Almost 87% of the species in this plot are with monopodial branching structure, which is marked with a main stem. D_{II} is under a crucial assumption that the intersection angle θ between branch and the main stem increases from top to bottom, averagely ranging from 0 deg to 90 deg.[48,49] Therefore, given the tree location and tree height, the point to a branch was able to be located and the branch distance D_{branch} and stem distance D_{stem} were calculated. The unscaled distance D_{I} is the contrast of scaled distance D_{II}.

D_{III} is the scaled linear distance from tree root to ALS point, scaled by tree height.

D_{IV} is the scaled distance along stem and branch based on crown center structure, scaled by tree height.

D_{V} is the scaled distance along branch based on crown center structure, scaled by tree height.

D_{VI} is the scaled distance along branch based on crown center structure, scaled by an assumed crown center height-related factor.

D_{VII} is the scaled distance along branch based on crown center structure, scaled by a regressive crown center height-related factor.

D_{IV}, D_{V}, D_{VI}, and D_{VII} are based on a strategy that the crown center is the distributing center of materials, i.e., the materials are transported from root to crown center and then to branches and leaves. The crown centers of D_{IV}, D_{V}, and D_{VI} are determined by λ, which stands for the proportion of crown center height to tree height. The crown center of D_{VII} is determined by regression equation as shown in Fig. 6. We tested a series of values λ ranging from 0.1 to 0.9.

D_{V}, D_{VI}, and D_{VII} employed branch distances but not stem distance. The scaling factors of D_{VI} and D_{VII} were based on the ratio of branch distance to crown radius, amplified by the power of n. For the ALS point inside of assumed or regressive crown radius, branch distance is smaller than crown distance, so the scaling factor $(D_{\mathrm{branchVI}}/r_{\mathrm{crownVI}})^n$ and $(D_{\mathrm{branchVII}}/r_{\mathrm{crownVII}})^n$ is smaller than 1 (Table 2), thus scaled distance is shorter than unscaled distance. For the ALS point outside of assumed or regressive crown radius, scaled distance is longer than unscaled distance. Therefore, ALS points belonging to the crown of understory will less likely to be

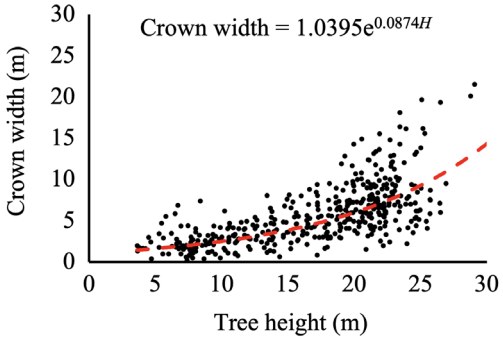

Fig. 6 The regression equation of crown width and tree height established based on true ALS, which were used for calculating the crown center height of D_{VII} = tree height – the half of crown width.

Table 2 Seven kinds of distances we developed, named as D_{I}, D_{II}, D_{III}, D_{IV}, D_{V}, D_{VI}, and D_{VII}.

Distance	Structure	Scaling factor[a]	Crown center height[b]	Expression[c]
D_{I}	Monopodial branching	1 (unscaled)	—	$D_{\mathrm{branchI}} + D_{\mathrm{stemI}}$
D_{II}	Monopodial branching	H^{-x}	—	$(D_{\mathrm{branchII}} + D_{\mathrm{stemII}}) \times H^{-x}$
D_{III}	—	H^{-x}	—	$D_{\mathrm{root}} \times H^{-x}$
D_{IV}	Crown center structure	H^{-x}	$\lambda \times H$	$(D_{\mathrm{branchIV}} + D_{\mathrm{stemIV}}) \times H^{-x}$
D_{V}	Crown center structure	H^{-x}	$\lambda \times H$	$D_{\mathrm{branchV}} \times H^{-x}$
D_{VI}	Crown center structure	$(D_{\mathrm{branchVI}}/r_{\mathrm{crownVI}})^n$	$\lambda \times H$	$D_{\mathrm{branchVI}} \times (D_{\mathrm{branchVI}}/r_{\mathrm{crownVI}})^n$, $n = 1,2,\mathrm{n}$
D_{VII}	Crown center structure	$(D_{\mathrm{branchVII}}/r_{\mathrm{crownVII}})^n$	Regressive (Fig. 6)	$D_{\mathrm{branchVII}} \times (D_{\mathrm{branchVII}}/r_{\mathrm{crownVII}})^n$, $n = 1,2,\ldots$

[a,b]The scaling factor and crown center height. The original unscaled distances were multiplied by the scaling factor. "1" stands for unscaled. H^{-x} stands for the tree height H to the power $-x$, where x was proved to be 2/3.[30,31,47] D_{branchVI} and $D_{\mathrm{branchVII}}$ were branch distances. r_{crownVI} and r_{crownVII} were the crown radii, and the crown center height and crown radius were determined by the parameter λ. For D_{VI}, $r_{\mathrm{crownVI}} = (1-\lambda) \times H$, where parameter λ was the proportion of crown center height to tree height. For D_{VII}, r_{crownVII} was obtained from the regression equation of tree height and crown radius (Fig. 5). Parameter n was a power factor ranging from 1 to 20.

[c]D_{branchI}, D_{branchII}, D_{branchIV}, D_{branchV}, D_{branchVI}, and $D_{\mathrm{branchVII}}$ are the transporting distances along branches, D_{stemI}, D_{stemII}, and D_{stemIV} are the transporting distances along stems. D_{root} is the linear distance between tree root and ALS point, where the horizontal coordinate of the tree root is assumed as that of treetop, which was already extracted during detection. Note that the branch distance is the linear distance between ALS point and crown center, and the stem distance is the linear distance between tree root and crown center.

falsely assigned to overstory or midstory compared with the comparison approaches, and this is the reason why our approach has the stronger ability to segment understories.

All seven different distances were applied separately to the segmentation process in terms of the tree locations and the initial tree height derived from detection.

2.5 *Assessment Method*

2.5.1 *Tree level assessment*

We assessed the detection and segmentation accuracy at tree level. If a real tree, extracted from true ALS (also TLS), exists and is detected by our approach, it is called true positive (TP); if a real tree exists but is not detected, it is called false negative (FN); if a real tree does not exist but a false tree is detected, then it is false positive (FP). We employed a searching threshold to determine whether a real tree is detected. If there is at least one tree extracted from our approach located within the area of radius searching threshold centered at the real tree, we judge the real tree is detected, otherwise the real tree is not detected. The radius threshold was set at a commonused value 3.0 m in this study. Also, recall (rec), precision (pre), and F-score (Fsc) were calculated as follows:[50–52]

$$\mathrm{rec} = \frac{\mathrm{TP}}{\mathrm{TP} + \mathrm{FN}}, \tag{1}$$

$$\mathrm{pre} = \frac{\mathrm{TP}}{\mathrm{TP} + \mathrm{FP}}, \tag{2}$$

$$\mathrm{Fsc} = \frac{2 \times \mathrm{rec} \times \mathrm{pre}}{\mathrm{rec} + \mathrm{pre}}. \tag{3}$$

It is recognized that higher TP, r, p, and F, with lower FN and FP indicate higher accuracy.[53–55] We also assessed the accuracy in both vertical and horizontal dimensions. For vertical dimension, we calculated the coefficient of determination (R^2) of tree height, and for horizontal dimension, we calculated R^2 of crown width. TP, FN, FP, rec, pre, and Fsc are aimed at assessing detection approach, whereas R^2 of tree height and crown width are aimed at assessing both detection and segmentation approaches.

Moreover, we assessed the performance of our approach and the comparison approaches according to three canopy layers: overstory, midstory, and understory. We employed the mean error of tree height (vertical) and crown width (horizontal) to measure the mean deviation of derived value from true value based on true ALS. This is especially aimed at testing the ability to delineate understories.

Table 3 Detection and segmentation accuracy assessment at tree and point-to-point levels. Top results with the percentage line threshold p varied from 32.0% to 34.0% were shown. The scaled transporting distance used for segmentation was D_{VI}, which was proved to be the best among the seven kinds of distances (Table 4). Note that TP value with 32.0%, 32.5%, and 33.5% are all 522, but different detected trees were matched, thus, the R^2 of height and crown width are different. Detected tree number with the value p of 100.0% (i.e., without the restriction of percentage line) was also listed.

p			32.0%	32.5%	33.0%	33.5%	34.0%	100.0%
Detection	Tree level	Detected tree numbers	595	575	554	544	529	63
		TP	522	522	523	522	520	—
		FN	1	1	0	1	3	—
		FP	73	53	31	22	9	—
		rec	1.00	1.00	1.00	1.00	0.99	—
		pre	0.88	0.91	0.94	0.96	0.98	—
		Fsc	0.93	0.95	0.97	0.98	0.99	—
		Height R^2	0.7720	0.7854	0.7784	0.7304	0.7328	—
		Crown width R^2	0.2119	0.2203	0.2075	0.1945	0.2036	—
		Height[a] R^2	0.8097	0.8210	0.7958	0.7951	0.7813	—
		Crown width[a] R^2	0.1601	0.1774	0.1440	0.1414	0.1532	—
	Point-to-point level	Truly assigned points	12,291	12,667	12,194	11,907	11,999	—
		Falsely assigned points	17,627	17,360	18,995	19,662	19,553	—
		Unassigned points	24,305	24,196	23,034	22,654	22,671	—
Segmentation	Tree level	Height R^2	0.7857	0.8045	0.7948	0.7543	0.7551	—
		Crown width R^2	0.4724	0.4743	0.4492	0.4259	0.4469	—
		Height[a] R^2	0.8191	0.8339	0.8108	0.8094	0.7991	—
		Crown width[a] R^2	0.4170	0.4144	0.3847	0.3759	0.3947	—
	Point-to-point level	Truly assigned points	18,591	19,212	18,964	18,773	19,127	—
		Falsely assigned points	16,049	16,646	15,796	16,085	15,629	—
		Unassigned points	19,583	18,365	19,463	19,365	19,467	—

[a]R^2 excluding 58 real trees without true ALS point, these trees were not matched with true ALS point but were manually segmented from TLS point cloud.

2.5.2 *Point-to-point level assessment*

We assessed the detection- and segmentation-based assignment accuracy at point-to-point level, as we have true ALS data, which were matched with TLS data. For a point, it could be truly assigned, falsely assigned, or unassigned. More truly assigned points, less falsely assigned and unassigned points indicate better assignment result. Detected tree numbers may be greater than real tree numbers, thus some detected trees will not be matched to any real tree, and the points of that detected trees will be unassigned points. Note that not all the points belonging to TP trees are truly assigned points, because some points belonging to crown edges of TP tree could be assigned to nearby trees.

To test the ability of our approach for detecting and segmenting understory, we also assessed the accuracy of three canopy layers, overstory, midstory, and understory, separately at the tree and point-to-point levels.

3 Results

3.1 *Performance of Tree Detection and Crown Segmentation*

3.1.1 *Tree and point level assessment*

We set a series of values of p ranging from 20.0% to 100.0% with an interval of 0.5% as the transporting distance threshold for individual tree detection, and each real tree was matched with the nearest detected tree within a search distance of 3 m. We assessed the accuracy of individual tree detection and crown segmentation at tree level, as shown in Table 3.

When parameter p is 32.0%, 32.5%, and 33.5%, there are the same numbers of 522 TP trees were detected, but corresponding R^2 of tree height and crown width were different. Because detected and segmented trees that were matched to the same tree were assigned with more or less different ALS points, so were those different in tree height and crown width.

The result of tree level assessment (Table 3) showed that the greater the value of p, the smaller the number of detected trees. The highest R^2 of tree height and crown width were reached when p equals 32.5%. The highest detection R^2 of height and crown width was 0.8210 and 0.2203, respectively, whereas the highest segmentation R^2 of height and crown width was 0.8339 and 0.4743, respectively. Compared with detection results, R^2 of tree height in segmentation results did not improve significantly, but R^2 of crown width was hugely improved. The reason lies in that the scaled distance-based segmentation approach is more powerful for delineating understories, as it was analyzed in Sec. 3.3 for the overstory, midstory, and understory.

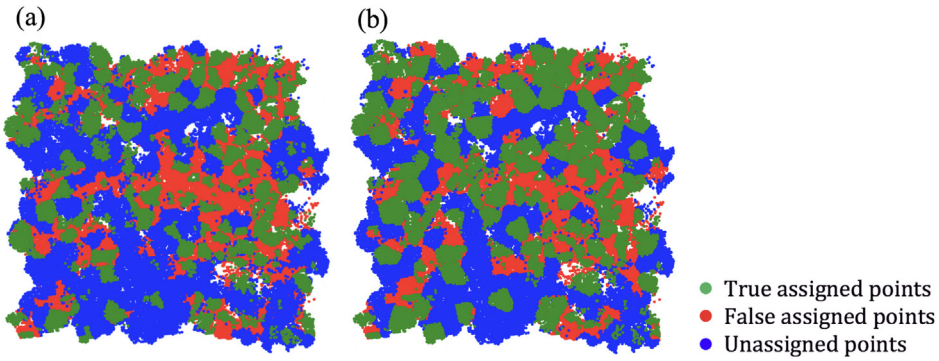

Fig. 7 Top view of (a) detection- and (b) segmentation-based assignment results based on transporting distance D_{VI}. Green, red, and blue points are truly assigned, falsely assigned, and unassigned ALS points, respectively.

3.1.2 *Point-to-point level assessment*

ALS points were assigned during detection and reassigned during segmentation, and more truly assigned points indicated better assignment result. When p equals 32.5%, the most truly assigned points of both detection and segmentation were achieved, as well as the highest R^2 of tree height and crown width. Schematic diagrams of assignment result were shown in Fig. 7.

There are 51.67% more truly assigned ALS points of segmentation-based assignment (19,212) than that of detection-based assignment (12,667). As for point-to-point level assignment, the scaled transporting distance-based segmentation performs better than the unscaled transporting distance-based detection. Thus, we reassigned points after detection. The detection

Table 4 Assessment of transporting distances. (a) Assessment of transporting distances D_{I}, D_{II}, and D_{III}. θ is the intersection angle between branch and stem. (b) Assessment of transporting distances D_{IV}, D_{V}, and D_{VI}. For D_{VI}, pilot tests were conducted where $n = 1,2,\ldots,20$; however, only the best result when $n = 8$ was listed. (c) Assessment of transporting distance D_{VII} ($n = 1,2,\ldots,20$). Only results when n is from 5 to 14 were listed.

(a)

Distance	D_{I}	D_{II}	D_{III}
θ	(0, 90)	(0, 90)	—
Height R^2	0.0010	0.6739	0.5620
Crown width R^2	0.1013	0.6919	0.5470
Truly assigned points	15,338	34,110	29,635

(b)

	λ	0.50	0.55	0.60	0.65	0.70	0.75	0.80	0.85	0.90	0.95
D_{IV}	Height R^2	0.7520	0.7687	0.7863	0.8464	0.8834	0.9127	0.9137	0.9073	0.8967	0.8746
	Crown width R^2	0.5533	0.5633	0.5752	0.5658	0.5599	0.5304	0.4803	0.4333	0.3569	0.2585
	Truly assigned points	34,476	34,826	34,976	34,981	34,576	33,747	32,477	30,661	28,258	24,938
D_{V}	Height R^2	0.7543	0.7579	0.7771	0.8098	0.8528	0.8946	0.9219	0.9294	0.9256	0.9210
	Crown width R^2	0.5627	0.5647	0.5757	0.5903	0.5908	0.5892	0.5794	0.5456	0.5103	0.4571
	Truly assigned points	33,557	34,060	34,574	34,922	35,181	35,076	34,471	33,617	31,922	29,567
D_{VI}	Height R^2	0.7178	0.7435	0.7935	0.8151	0.8407	0.8934	0.9108	0.9256	0.9147	0.8832
	Crown width R^2	0.5480	0.5525	0.5792	0.5978	0.5980	0.6005	0.6193	0.6007	0.5432	0.4558
	Truly assigned points	32,812	33,524	34,184	34,823	35,184	35,218	34,695	33,106	26,804	11,699

(c)

n	5	6	7	8	9	10	11	12	13	14
Height R^2	0.9296	0.9271	0.9283	0.9289	0.9271	0.9247	0.9253	0.9276	0.9297	0.9276
Crown width R^2	0.5524	0.5621	0.5703	0.5813	0.5809	0.5818	0.5805	0.5803	0.5764	0.5747
Truly assigned points	33,882	33,871	33,795	33,630	33,338	32,889	32,308	31,660	31,053	30,407

approach aims at searching for tree stems and deriving tree height, whereas the segmentation approach aims at delineating crown edge.

3.2 *Performance of True Tree Location-Based Segmentation*

To evaluate the performance of segmentation approach based on the proposed seven kinds of transporting distances, the influence of detection approach was removed by segmenting crowns based on true tree locations, instead of detected tree locations. Accuracy assessment was done using R^2 of tree height and crown width and truly assigned points as shown in Table 4.

The validation data in Table 4, including true height and crown width used for calculating R^2, were derived from true ALS data, instead of TLS data. Tree and point-to-point level assessment showed that D_{VII} has the highest R^2 of height 0.9289, D_{II} has the highest R^2 of crown width 0.6919, and D_{VI} has the highest number of truly assigned points 35,218. However, the optimal transporting distance strategy is D_{VI} with $n = 8$ and $\lambda = 0.80$, which contributed to comprehensive results in height R^2 of 0.9108, tree crown R^2 of 0.6193, and truly assigned points of 34,695. Moreover, D_{VI} performed better than other distance strategies at both tree and point-to-point levels. Therefore, the detection processing was based on the unscaled D_{VI} (i.e., the scaling factor equaled one), and segmentation processing was based on scaled D_{VI}.

In Fig. 8, it can be seen that there is obvious overestimated height under the strategy of D_{I} and obvious underestimated height under strategies of D_{II} and D_{III}. The unscaled distance D_{I} based on a monopodial branching structure assigned more points to understory and added the derived tree heights. On the contrast, the transporting distances D_{IV}, D_{VI}, and D_{VII} performed better, and there was less over- or underestimation. It can be further confirmed from the top views of assigned ALS point cloud in Fig. 9.

3.3 *Performance of Our Approach and Comparison Approaches of Different Canopy Layers*

Three commonly used approaches for tree detection and crown segmentation were also applied to the 1-ha plot as comparison approaches, including CHM-based (CHM), pit-free CHM-based (PFCHM), and point cloud – layer stacking seed point-based (PCLSS) approaches.[10,20,56,57] CHM and PFCHM are typical CHM-based method, whereas PCLSS is typical point cloud-based method.

The CHM approach used a CHM-based watershed algorithm and CHM was generated from raw point cloud,[19,58,59] the PFCHM approach also used a watershed algorithm but based on the pit-free CHM generated by removing pit from CHM,[60] and PCLSS approach combined the

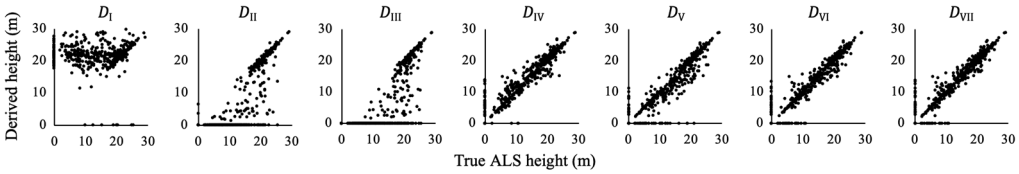

Fig. 8 Scatter diagrams of true tree height and true tree location-based segmentation height. D_{IV} was with $\lambda = 0.75$, D_{V} was with $\lambda = 0.80$, and D_{VI} was with $\lambda = 0.80$, $n = 8$.

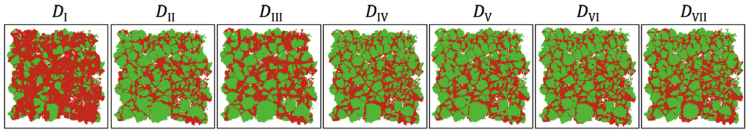

	D_{I}	D_{II}	D_{III}	D_{IV}	D_{V}	D_{VI}	D_{VII}
Correct assigned points (%)	28.29%	62.91%	54.65%	62.24%	64.88%	63.99%	60.66%
Incorrect assigned points (%)	71.71%	37.09%	45.35%	37.76%	35.12%	36.01%	39.34%

Fig. 9 Top views of assigned ALS point cloud. Green points are correctly assigned, red points are incorrectly assigned and the percentage were also listed.

regional growth and spacing threshold[3] with the layer stacking algorithm.[61] As the performance of the approaches shown in Fig. 10, all three comparison approaches overestimated tree heights, the CHM and PFCHM approach missed most of the information of understories, whereas the PCLSS approach falsely assigned large amount of ALS points to understories such as D_I (Fig. 8). The crown width R^2 of all the three comparison approaches were <0.1, in contrast to 0.4743 generated in the D_{VI}-based approach in this study.

CHM and PFCHM approaches were CHM-based approaches and did not segment the raw point cloud, thus we cannot assess the accuracy at point-to-point level. PCLSS approach segmented the raw point cloud, and the point-to-point level result was shown in Fig. 11. Truly assigned point numbers from PCLSS approach (17,516) were greater than those of detection result (12,667, see Table 3 with $p = 32.5\%$) and were less than those of segmentation result (19,212), and the derived height R^2 ($< = 0.2$) was less than detection result (0.8210) or segmentation result (0.8339). This showed that at point-to-point level, the segmentation approach developed in this study performed better than PCLSS approach, especially in targeting the understories.

The tree height based on true ALS ranges from 2.23 to 30.19 m. We divided the trees into three canopy layers: overstory (tree height ≥ 20 m), midstory (10 to 20 m), and understory (≤10 m) (Table 1) and assessed the accuracy of our approach and three comparison approaches for different canopy layers as shown in Fig. 12.

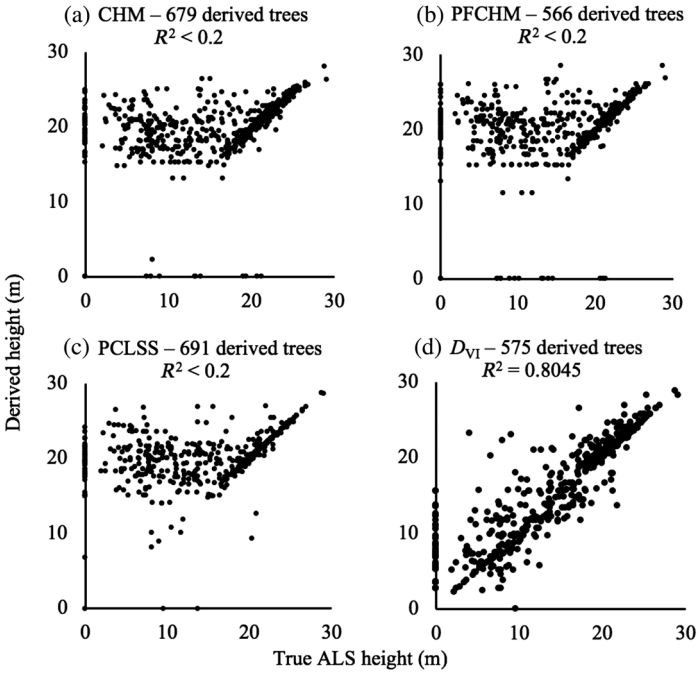

Fig. 10 Scatter diagrams of true ALS tree height and derived tree height of the three comparison approaches: (a) CHM approach, (b) PFCHM approach, (c) PCLSS approach, and (d) the transporting distance D_{VI}-based approach. Only the best result of each approach was provided among a series of parameters as follows. (a) Resolution of CHM was 0.3 m, Gaussian smoothing factor was 1.7, Gaussian smoothing radius was seven pixels, and derived tree numbers were 679. (b) Resolution of CHM was 0.3 m, Gaussian smoothing factor was 1.3, Gaussian smoothing radius was seven pixels, and derived tree numbers were 566. (c) Spacing threshold was 1.0 m, Gaussian smoothing factor was 1.7, Gaussian smoothing radius was 15 pixels, and derived tree numbers were 691. (d) Ratio λ of crown center height over tree height was 0.80, percentage line p was 32.5%, power n was 8, and derived tree numbers were 575. All the R^2 of tree height of the three comparison approaches are <0.2 due to the obvious overestimation of understory. The 58 dots that fell on the y-axis are the understories, which were not assigned with any ALS point, and we marked the height as 0 m. Similarly, the dots that fell on the x-axis are the trees that were not assigned with any ALS point by the approach and were marked as 0 m height.

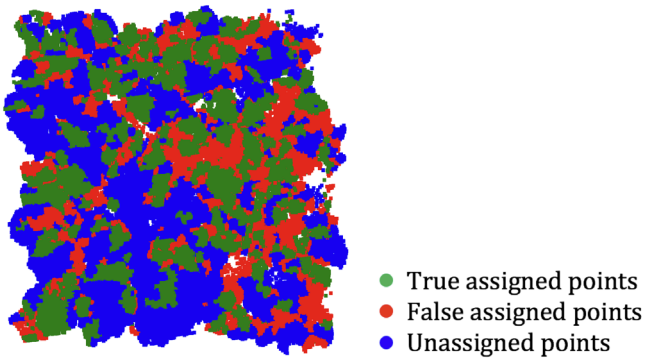

Fig. 11 Top view of point-to-point level assessment of PCLSS approach [Fig. 10(c)] in comparison with the results generated in this study (Fig. 7). Green, red, and blue points are 17,516 (32.3%) truly assigned, 13,534 (25.0%) falsely assigned, and 23,173 (42.7%) unassigned ALS points, respectively.

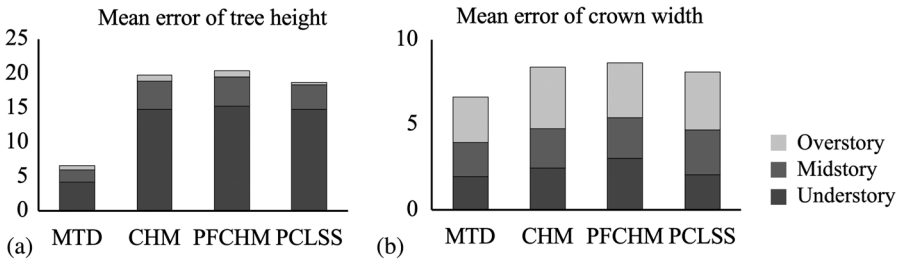

Fig. 12 Histograms of mean errors of (a) tree height and (b) crown width obtained in our approach (MTD) and three comparison approaches for overstory, midstory, and understory. The mean error is the average absolute difference of derived value based on algorithms and true value based on true ALS.

The accuracy assessment of different canopy layers (Fig. 12) showed that our approach has the better ability to segment individual trees, especially to extract tree heights compared with other CHM- and point-based approaches. The mean error of tree height of all layers based on our approach is 2.20 m, whereas that of comparison approaches ranges from 6.24 to 6.58 m. It is the same for the mean value of crown width. For understory, our approach showed great potential to correctly delineate trees. Our approach has the error of understory tree height of 4.19 m, whereas the other comparison approaches have more than three times of errors, ranging from 14.82 to 15.21 m, which showed a great overestimation by assigning too many top-height points to the understories. Our approach employed the transporting distance to reduce the overestimation by removing high points from understories. For the crown width, our approach (D_{VI}) is more powerful to delineate the crown edge by enlarging the transporting distance of the point out of assumed crown (Table 2, D_{VI}).

Compared with the typical CHM-based approaches (CHM and PFCHM) and point cloud-based approach (PCLSS), the MTD -based approach we developed performed well in delineating individual trees, especially for understories. According to the tree level assessment, R^2 of tree height and crown width, the newly developed approach performed better (0.8045 and 0.4743, respectively) than the three comparison approaches (all <0.2 and 0.1, respectively). According to the point-to-point level assessment, the general performance of newly developed segmentation approach (19,212 truly assigned points) is superior to the point cloud-based approach, PCLSS (17,516 truly assigned points).

4 Discussion

Almost all segmentation approaches employed at least one parameter to control the detected results, and the parameter affected the results in varying degrees. For the compared CHM-based

approaches we used, the performance is affected by the resolution of CHM, the Gaussian smoothing factor and radius (see title of Fig. 10). For the compared point cloud-based approach we used, the performance is affected by the spacing threshold, Gaussian smoothing factor, and radius (Fig. 10). As with comparison approaches, our approach has two parameters, the ratio λ of crown center height over tree height, which determines the crown center height, and percentage line value p, which determines the threshold of unscaled distance during stem detection. For transporting distance D_{VI}, when parameter p varies from 32.0% to 34.0% (Table 3), parameter λ varies from 0.70 to 0.90 [Table 4(b)], the R^2 value of tree level assessment fluctuates within 0.1, and no more than 2% of truly assigned points were reassigned. Therefore, from the sensitivity analysis, the segmentation result based on distance D_{VI} is not sensitive to parameters p varying from 32.0% to 34.0% and λ varying from 0.70 to 0.90. In addition, according to the accuracy assessment above, it is recommended to set parameter p and λ at 32.50% to 33.50% and 0.75 to 0.85, respectively.

The ability of detecting and extracting understories of this approach is shown in Fig. 13. In Fig. 13(b), orange points were assigned to tree 8, with lots of blue points alternate. The alternate blue points will be assigned to other trees that are with shorter transporting distance than tree 8. However, CHM-based approaches will assign all the points (pixels) within this area to one individual tree.

Ascendingly ordered distributions of derived tree height (Fig. 14) also demonstrated the ability of our approach in delineating the understory. The three comparison approaches (CHM, PFCHM, and PCLSS) obviously overestimated tree height, especially for the first 300 short trees, which were 5.6, 6.0, and 6.1 m on average, respectively. By contrast, the detection and segmentation height overestimated by 2.0 and 1.4 m, respectively. This suggested that the MTD -based approach can greatly reduce the overestimation of understory.

However, the transporting distances D_I and D_{II} are based on the monopodial structure, which limits the implementation to the nonmonopodial structured forest. Also, the branching angles of the monopodial structured trees differ from specific species. Moreover, we only implemented the approach to deciduous forest, which is with medium complexity of canopy layers, and further attempt in tropical forest or coniferous forest is needed, and corresponding sensitivity analysis should also be carried out. But it can be estimated that it is more difficult in implementation on tropical forests than on coniferous forests due to the complexity of the canopy layers of forests. As for the influence of point density, it is predictable that a higher point density data could offer more detailed structure of overstories, as well as of understories, thus, the approach could find treetops and trace the paths more accurately, and vice versa. Also, the training data are necessary for the determination of parameter p (Fig. 4), which will affect the individual tree detection and will further affect the crown segmentation, thus, it is important in selecting training data in further study.

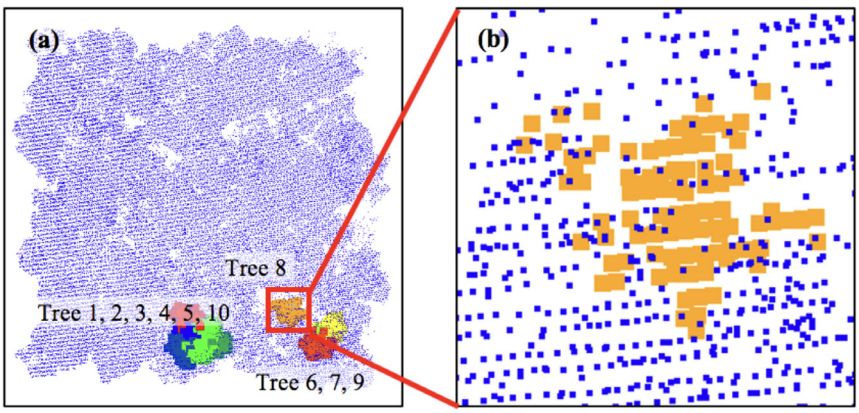

Fig. 13 Diagram of the first 10 detected trees using unscaled transporting distance-based top-to-bottom detection approach in the 1-ha plot, and the 10 trees are sequentially named with tree 1, 2, . . . , 10. (a) Each color excluding blue stands for an individual tree. (b) A local enlarged drawing of tree 8.

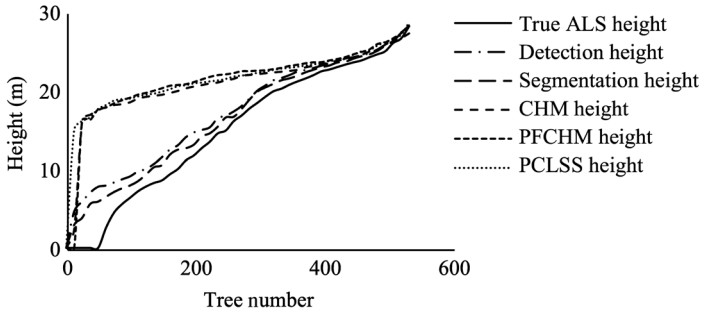

Fig. 14 Distribution of extracted height of trees. The height of each line was in ascending order. Six lines stand for true ALS derived height, detection derived height, segmentation derived height, and three comparison approaches derived height.

5 Conclusions

We presented a new approach that applied an MTD theory to detect individual trees and segment tree crowns from ALS point cloud. The foundation is that vascular plants tend to minimize the material transporting distance from root to leaves. To trace the transporting path, we developed monopodial branching structure-based distances (D_{I} and D_{II}) and crown center-based distances (D_{IV}, D_{V}, D_{VI}, and D_{VII}). The experiments are based on ALS data acquired in a 1-ha deciduous forest, and we assessed the accuracy at both tree level and point-to-point levels.

Mapping results from our approach are compared with two commonly used CHM- and one point cloud-based approaches available from known software packages. Results showed that our approach performed well in both detecting trees and segmenting crowns. Compared with the three comparison approaches, our approach greatly reduced the errors in retrieving tree height and crown width of understories and worked better in the understory of forest because of its superiority in delineating small trees. Moreover, according to sensitive analysis, our approach is less sensitive to the two key control parameters, λ and p. This showed that MTD theory was successfully applied in individual tree detection and tree crown segmentation from ALS point cloud.

Acknowledgments

This research was funded under the Metrology for Earth Observation and Climate project (MetEOC-2) and the European Metrology Research Programme (EMRP, Grant No ENV55). EMRP is jointly funded by the EMRP participating countries within EURAMET and the European Union. This work was supported by the China Scholarship Council (Grant No. 201906010036); the Open Research Fund of Key Laboratory of Digital Earth Science, Institute of Remote Sensing and Digital Earth, Chinese Academy of Sciences (Grant No. 2017LDE007); and the National Natural Science Foundation of China (Grant No. 31870531).

References

1. K. Lim et al., "Lidar remote sensing of forest structure," *Prog. Phys. Geogr.* **27**(1), 88–106 (2003).
2. S. Briechle, P. Krzystek, and G. Vosselman, "Semantic labeling of ALS point clouds for tree species mapping using the deep neural network PointNet++," *Int. Arch. Photogramm. Remote Sens. Spatial Inf. Sci.* **XLII-2/W13**, 951–955 (2019).
3. Y. Lin et al., "Recruiting conventional tree architecture models into state-of-the-art lidar mapping for investigating tree growth habits in structure," *Front. Plant Sci.* **9**, 220 (2018).
4. M. Parkan and D. Tuia, "Estimating uncertainty of point-cloud based single-tree segmentation with ensemble based filtering," *Remote Sens.* **10**(2), 335 (2018).
5. A. Persson, J. Holmgren, and U. Soderman, "Detecting and measuring individual trees using an airborne laser scanner," *Photogramm. Eng. Remote Sens.* **68**(9), 925–932 (2002).

6. Q. Chen et al., "Estimating basal area and stem volume for individual trees from lidar data," *Photogramm. Eng. Remote Sens.* **73**(12), 1355–1365 (2007).
7. J. W. Roberts et al., "Forest structural assessment using remote sensing technologies: an overview of the current state of the art," *Southern Hemisphere For. J.* **69**(3), 183–203 (2007).
8. M. Van Leeuwen and M. Nieuwenhuis, "Retrieval of forest structural parameters using lidar remote sensing," *Eur. J. For. Res.* **129**(4), 749–770 (2010).
9. J. Williams et al., "3D segmentation of trees through a flexible multiclass graph cut algorithm," *IEEE Trans. Geosci. Remote Sens.* **58**, 754–776 (2019).
10. Q. Yang et al., "The influence of vegetation characteristics on individual tree segmentation methods with airborne lidar data," *Remote Sens.* **11**(23), 2880 (2019).
11. A. Ferraz et al., "Canopy density model: a new ALS-derived product to generate multilayer crown cover maps," *IEEE Trans. Geosci. Remote Sens.* **53**(12), 6776–6790 (2015).
12. D. A. Coomes et al., "Area-based vs tree-centric approaches to mapping forest carbon in Southeast Asian forests from airborne laser scanning data," *Remote Sens. Environ.* **194**, 77–88 (2017
13. S. Xu et al., "A supervoxel approach to the segmentation of individual trees from lidar point clouds," *Remote Sens. Lett.* **9**(6), 515–523 (2018).
14. M. Aubry-Kientz et al., "A comparative assessment of the performance of individual tree crowns delineation algorithms from ALS data in tropical forests," *Remote Sens.* **11**(9), 1086 (2019).
15. F. Morsdorf et al., "Clustering in airborne laser scanning raw data for segmentation of single trees," *Int. Arch. Photogramm. Remote Sens. Spatial Inf. Sci.* **34**(part 3), W13 (2003).
16. N. Amiri et al., "Adaptive stopping criterion for top-down segmentation of ALS point clouds in temperate coniferous forests," *ISPRS J. Photogramm. Remote Sens.* **141**, 265–274 (2018).
17. W. Li et al., "A new method for segmenting individual trees from the lidar point cloud," *Photogramm. Eng. Remote Sens.* **78**(1), 75–84 (2012).
18. M. Dalponte and D. A. Coomes, "Tree-centric mapping of forest carbon density from airborne laser scanning and hyperspectral data," *Methods Ecol. Evol.* **7**(10), 1236–1245 (2016).
19. Z. Hou et al., "Extraction of remote sensing-based forest management units in tropical forests," *Remote Sens. Environ.* **130**, 1–10 (2013).
20. J. H. Hastings et al., "Tree species traits determine the success of lidar-based crown mapping in a mixed temperate forest," *Remote Sens.* **12**(2), 309 (2020).
21. M. Dalponte et al., "Tree crown delineation and tree species classification in boreal forests using hyperspectral and ALS data," *Remote Sens. Environ.* **140**, 306–317 (2014).
22. J. Lee et al., "A graph cut approach to 3D tree delineation, using integrated airborne lidar and hyperspectral imagery," arXiv:1701.06715 (2017).
23. T. L. Swetnam and D. A. Falk, "Application of metabolic scaling theory to reduce error in local maxima tree segmentation from aerial lidar," *For. Ecol. Manage.* **323**, 158–167 (2014).
24. M. Vehmas et al., "Using airborne laser scanning data for detecting canopy gaps and their understory type in mature boreal forest," *Ann. For. Sci.* **68**(4), 825–835 (2011).
25. S. Tao et al., "Segmenting tree crowns from terrestrial and mobile lidar data by exploring ecological theories," *ISPRS J. Photogramm. Remote Sens.* **110**, 66–76 (2015).
26. B. J. Enquist, "Cope's rule and the evolution of long-distance transport in vascular plants: allometric scaling, biomass partitioning and optimization," *Plant Cell Environ.* **26**(1), 151–161 (2003).
27. V. M. Savage et al., "Hydraulic trade-offs and space filling enable better predictions of vascular structure and function in plants," *Proc. Natl. Acad. Sci. U. S. A.* **107**, 22722–22727 (2010).
28. C. P. Kempes et al., "Predicting maximum tree heights and other traits from allometric scaling and resource limitations," *PLoS One* **6**(6), e20551 (2011).
29. L. B. Leopold, "Trees and streams: the efficiency of branching patterns," *J. Theor. Biol.* **31**(2), 339–354 (1971).
30. G. B. West, J. H. Brown, and B. J. Enquist, "A general model for the structure and allometry of plant vascular systems," *Nature* **400**(6745), 664–667 (1999).

31. B. J. Enquist, "Universal scaling in tree and vascular plant allometry: toward a general quantitative theory linking plant form and function from cells to ecosystems," *Tree Physiol.* **22**(15-16), 1045–1064 (2002).
32. T. L. Swetnam et al., "Estimating individual tree mid-and understory rank-size distributions from airborne laser scanning in semi-arid forests," *For. Ecol. Manage.* **330**, 271–282 (2014).
33. N. Butt et al., *Initial Results from Establishment of a Long-Term Broadleaf Monitoring Plot at Wytham Woods*, University of Oxford Report, Oxford (2009).
34. K. Calders et al., "Realistic forest stand reconstruction from terrestrial lidar for radiative transfer modeling," *Remote Sens.* **10**(6), 933 (2018).
35. K. Calders et al., "Large-area virtual forests from terrestrial laser scanning data," in *IEEE Int. Geosci. Remote Sens. Symp. (IGARSS)*, pp. 1765–1767 (2016).
36. X. Zhao et al., "Improved progressive TIN densification filtering algorithm for airborne lidar data in forested areas," *ISPRS J. Photogramm. Remote Sens.* **117**, 79–91 (2016).
37. Green Valley International, "LiDAR360," 2021, https://greenvalleyintl.com/software/lidar360/.
38. Q. Chen, "Airborne lidar data processing and information extraction," *Photogramm. Eng. Remote Sens.* **73**(2), 109–112 (2007).
39. K. A. Razak et al., "Generating an optimal DTM from airborne laser scanning data for landslide mapping in a tropical forest environment," *Geomorphology* **190**, 112–125 (2013).
40. R. Gaulton and T. J. Malthus, "Lidar mapping of canopy gaps in continuous cover forests: a comparison of canopy height model and point cloud based techniques," *Int. J. Remote Sens.* **31**(5), 1193–1211 (2010).
41. B. Hu et al., "Improving the efficiency and accuracy of individual tree crown delineation from high-density lidar data," *Int. J. Appl. Earth Obs. Geoinf.* **26**, 145–155 (2014).
42. M. Mielcarek, K. Stereńczak, and A. Khosravipour, "Testing and evaluating different lidar-derived canopy height model generation methods for tree height estimation," *Int. J. Appl. Earth Obs. Geoinf.* **71**, 132–143 (2018).
43. rapidlasso GmbH, "LAStools," 2021, http://rapidlasso.com/lastools/.
44. Guido van Rossum, "Python," 2021, http://www.python.org.
45. A. Ferraz et al., "3-D mapping of a multi-layered Mediterranean forest using ALS data," *Remote Sens. Environ.* **121**, 210–223 (2012).
46. H. Hamraz, M. A. Contreras, and J. Zhang, "Vertical stratification of forest canopy for segmentation of understory trees within small-footprint airborne lidar point clouds," *ISPRS J. Photogramm. Remote Sens.* **130**, 385–392 (2017).
47. L. P. Bentley et al., "An empirical assessment of tree branching networks and implications for plant allometric scaling models," *Ecol. Lett.* **16**(8), 1069–1078 (2013).
48. D. A. King, "Relationship between crown architecture and branch orientation in rain forest trees," *Ann. Bot.* **82**(1), 1–7 (1998).
49. P. Kruszewski, "An algorithm for sculpting trees," *Comput. Graphics* **23**(5), 739–749 (1999).
50. C. Goutte and E. Gaussier, "A probabilistic interpretation of precision, recall and F-score, with implication for evaluation," in *Eur. Conf. Inf. Retrieval*, Springer, Berlin, Heidelberg, pp. 345–359 (2005).
51. M. Sokolova, N. Japkowicz, and S. Szpakowicz, "Beyond accuracy, F-score and ROC: a family of discriminant measures for performance evaluation," in *Australasian Joint Conf. Artif. Intell.*, Springer, Berlin, Heidelberg, pp. 1015–1021 (2006).
52. F. Pirotti, M. Kobal, and J. R. Roussel, "A comparison of tree segmentation methods using very high density airborne laser scanner data," *Int. Arch. Photogramm. Remote Sens. Spatial Inf. Sci.* **42**, 1015–1021 (2017).
53. C. Véga et al., "PTrees: a point-based approach to forest tree extraction from lidar data," *Int. J. Appl. Earth Obs. Geoinf.* **33**, 98–108 (2014).
54. D. Yin and L. Wang, "How to assess the accuracy of the individual tree-based forest inventory derived from remotely sensed data: a review," *Int. J. Remote Sens.* **37**(19), 4521–4553 (2016).
55. J. C. Carr and J. B. Slyder, "Individual tree segmentation from a leaf-off photogrammetric point cloud," *Int. J. Remote Sens.* **39**(15–16), 5195–5210 (2018).

56. P. H. K. Millikan et al., "Automated individual tree detection in Amazon tropical forest from airborne laser scanning data," *CERNE* **25**(3), 273–282 (2019).
57. A. Zaforemska, W. Xiao, and R. Gaulton, "Individual tree detection from UAV lidar data in a mixed species woodland," in *ISPRS Geospatial Week 2019* (2019).
58. J. Pitkänen et al., "Adaptive methods for individual tree detection on airborne laser based canopy height model," *Int. Arch. Photogramm. Remote Sens. Spatial Inf. Sci.* **36**(8), 187–191 (2004).
59. P. Soille, *Morphological Image Analysis: Principles and Applications*, Springer Science & Business Media (2013).
60. A. Khosravipour et al., "Generating pit-free canopy height models from airborne lidar," *Photogramm. Eng. Remote Sens.* **80**(9), 863–872 (2014).
61. E. Ayrey et al., "Layer stacking: a novel algorithm for individual forest tree segmentation from lidar point clouds," *Can. J. Remote Sens.* **43**(1), 16–27 (2017).

Honglu Xin is a PhD student at the Institute of Remote Sensing and Geographic Information Systems, School of Earth and Space Science, Peking University, Beijing, China. His current research interest includes ecological remote sensing.

Yadvinder Malhi is a professor of ecosystem science at the School of Geography and the Environment, and the program leader of the Ecosystems Group at the Environmental Change Institute, University of Oxford, United Kingdom. His research interests focus on understanding the functioning of ecosystems and how it is altered by processes of local and global change. He has a particular interest in tropical forests, but has recently been frequently sighted in polar regions.

David A. Coomes is a professor in the Department of Plant Sciences, University of Cambridge, United Kingdom. His is interested in understanding how humans are changing the world's forests and how we can reduce impacts. Focusing on forest conservation and ecology, his research uses large databases and modern computational approaches, alongside traditional field approaches.

Yi Lin received his PhD in photogrammetry and remote sensing from Peking University, Beijing, China. He is currently a research professor with the School of Earth and Space Sciences, Peking University. His research interests include LiDAR remote sensing, earth interaction, and earth observation.

Baoli Liu received her PhD from the School of Geography, University of Hull, United Kingdom, in 2015. Currently, she is a research professor at the Institute of Binjiang, Zhejiang University, China. Her research interests include geomorphology and geostatistics.

Qiuli Yang is currently a PhD student at the Institute of Botany, Chinese Academy of Sciences, Beijing, China. Her research focuses on using multisource remote sensing data to derive forest structural parameters and functional parameters.

Alexander Shenkin is a postdoctoral researcher in the Ecosystems Group at the Environmental Change Institute, University of Oxford, United Kingdom. His research focuses on how tropical forests respond to drivers such as drought, logging, fire, and climate change.